PART 1

SOLAR UV VARIABILITY

Richard F. Donnelly

NOAA Air Resources Laboratory, Boulder, Colorado, U.S.A.

UV TRIAD

A new era in research of the temporal variations of solar UV radiation started on Nov. 7, 1978, with nearly daily measurements of the relative temporal variations of the solar UV flux in the 160 - 400 nm wavelength range by the Solar Backscatter Ultraviolet (SBUV) instrument on the NIMBUS7 satellite (HEATH, 1980). Similar SBUV/2 monitors have been operating on NOAA9 since April 1985 (DONNELLY, 1988b) and on NOAA11 since Nov. 1988, and are scheduled to fly on several more future NOAA satellites. The SBUV measurements form one part of a triad that is providing a major improvement in our understanding of solar UV flux variations.

The second part of the triad is the independent measurement of the solar UV flux in the 115 - 305 nm range from the SME satellite starting in October 1981 (ROTTMAN et al., 1982), which is still operating. A similar instrument is scheduled to fly on the UARS satellite in late 1991 as well as a SUSIM instrument (VANHOOSIER et al., 1981). These instruments are optimized for solar observations and include in-flight calibrations and reference components that are not routinely exposed to the space environment and solar UV radiation in order to detect instrument drift in the components used to make the daily measurements.

The triad's third part involves modeling the full-disk UV flux from spatially resolved measurements of solar activity (LEAN et al., 1982). This complements the corroborating measurements by providing a better physical understanding of why the UV variations have their observed temporal and wavelength dependences. Currently, quite crude scaled data of plage areas, brightness and location are used while an evolution toward more quantitative spatially-scanned data in the Ca K line from ground-based observatories is in progress.

UV instruments flown in space usually have problems with instrumentation drifts. Besides in-flight calibrations, rarely exposed reference components, occasional heating of some optical components to drive off surface contaminants and stowing of optical components when not in use, two other approaches to determine long-term variations are being used, namely: (1) relative photometry to increase long-term relative precision, like the Mg II core-to-wing ratio (HEATH and SCHLESINGER, 1986) and (2) shuttle-flight measurements of the solar UV spectral irradiance with excellent absolute flux accuracy using both SUSIM and also Simon's UV section of the European Spacelab instrument (LABS et al., 1987). These latter measurements are sometimes referred to as re-calibration measurements for the satellite monitors; or the satellite measurements may be viewed as providing the short-term (days, weeks) and intermediate-term (months) relative variations in the vicinity of these shuttle flight measurements to aid the interpretation of the long-term (years, solar cycle) changes.

SOLAR CYCLE VARIATIONS

Figure 1 shows several long-term trends during solar cycle 21. The measurements of the total solar irradiance (S) show daily data where the narrow lines extending 0.1 to 0.2% below the longer-term trend are dips caused by sunspot darkening and the long-term decline is interpreted as a decrese in

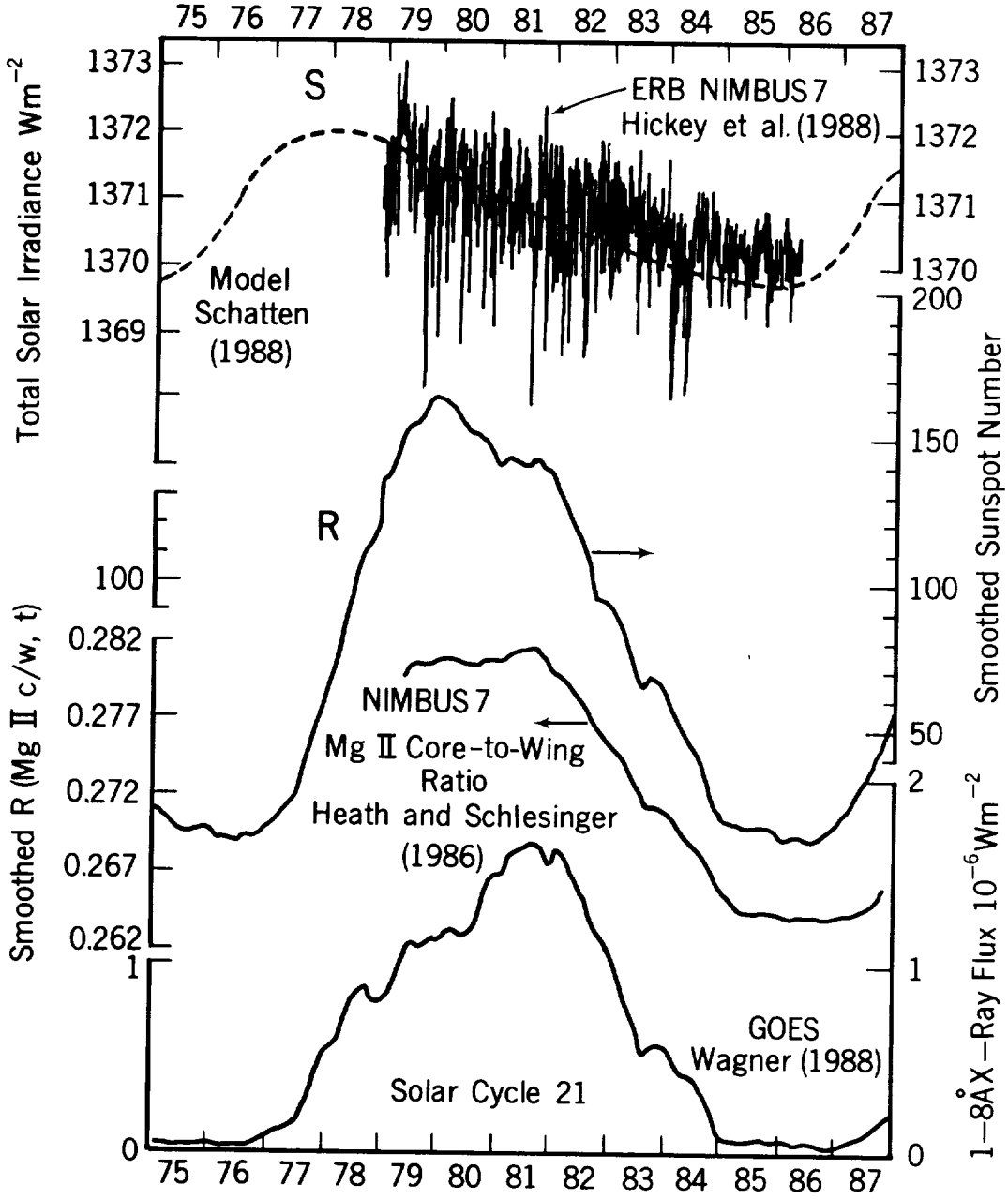

Figure 1. Solar cycle variations for the total irradiance, sunspot number, Mg II and soft X-rays. The bottom three curves are monthly values of annually smoothed data.

white-light facula brightening. The measurements suggest that the long-term maximum occurs either in early 1979 or before the measurements started. Either way, S peaks distinctly before the cycle maxima for the other three curves. Schatten's model for S(t) places the maximum for S almost two years earlier than that for the sunspot number (R). His model stresses the importance of the high contrast for white-light faculae at large solar central angles (60 - 90°) and such low contrast at small central angles (0 - 30°) that it is difficult to observe or detect faculae near the center of the disk. Schatten's model includes polar faculae, which have high central angles, contributing a peak effect after solar minimum, during the fast rise and early peak of his S(t) model. Also, the butterfly diagram of solar activity shows that regions tend to emerge at higher solar latitudes early in the cycle (30°) and progress toward the solar equator at the end of the cycle; so the contrasts of facula tend to be higher early in the cycle because their solar central angles are higher on average during their apparent passage across the solar disk. Conversely, sunspots have their maximum darkening as seen at Earth when they are at small solar central angles. Thus the solar cycle dependence of the active latitudes coupled with the white light contrasts for facula brightening and sunspot darkening and foreshortening of areas as a function of central angle cause the peak of the solar cycle dependence of S to occur earlier than for chromospheric and photospheric UV fluxes. Considering that the UV fluxes are not a negligible portion of S(t), and that the UV flux peaks later in the cycle, future revised models for S(t) will probably not peak quite as early as the dashed curve in Figure 1. Nevertheless, S appears to have a dull saw tooth appearance with a fast rise, early blunt peak and long slow decay with numerous narrow cracks caused by sunspot darkening.

The sunspot number R peaks in late 1979, about two years earlier than the UV flux; however R is strongly dominated by the number of groups of sunspots. The number of sunspots, excluding the number of groups, peaks about two years later than R and has a flatter peak (WILSON et al., 1987), which is more like the Mg II UV data in Figure 1. The chromospheric and upper photospheric UV flux variations caused by active regions are only weakly influenced by dark sunspots, filaments, etc., and are dominated by bright plages, plage remnants and numerous small active network features (LEAN et al., 1982). The solar central angle dependence of these features, combining contrast and foreshortening, has a fairly flat peak at small central angles or at the center of the sun viewed at Earth, dropping to about 40% near 60° and near zero at the limb (90°). This makes the solar UV flux at Earth slightly less sensitive to the high latitude regions at the start of a new cycle but fairly insensitive to the latitudes of the regions throughout the rest of the cycle. Note that the shape of the solar cycle curve for the UV Mg II ratio is fairly flat in 1985 and 1986.

The soft X-ray flux has a much higher peak in late 1981 than its level in late 1979 than do the UV fluxes observed by NIMBUS7 in the 170 - 300 nm range. This implies the net emission measure of hot cornal plasma at $T > 3 \times 10^6$ °K is significantly higher in late 1981, which implies higher emission of the coronal Fe XV line at 284 A and Fe XVI line at 335 A in late 1981 than in late 1979. RYBANSKI et al. (1988) showed that the Fe XIV green line coronal index also has a much higher long-term peak in late 1981 than in late 1979. Although AE-E measurements of the Fe XV and XVI EUV lines in 1977-1980 were closely correlated with the Ottawa 10.7 cm flux (F10) during the early rise of solar cycle 21, these soft X-ray and green line results imply the AE-E measurements significantly missed the solar cycle peak fluxes for EUV coronal lines. F10, which will be shown below to have a solar cycle shape like that for the chromospheric Mg II data, does not have a solar cycle shape like that for the coronal soft X-ray flux and green line; therefore, F10 does not represent well the temporal

shape of solar cycle variations of coronal emissions. In Figure 1, note the low flat levels at solar cycle minimum for the soft X-rays in 1975, 1976, 1985 and 1986, i. e. the hot coronal emission ($T > 3x10^6$ K) drops to negligible low levels for about two years at the solar cycle minimum.

The main purpose of Figure 1 is to illustrate that the solar cycle shape of solar fluxes and activity indices varies from an early peak in S(t) to much later peaks in the UV flux and soft X-rays. Secondly, the ratio of the maximum flux to minimum is about 0.1% for S(t), 7% for the UV Mg II core-to-wing ratio to more than 85x's for the 1 - 8 A soft X-rays for annually smoothed data.

Figure 2 shows daily values of F10 (the best of the currently available ground-based daily measures of solar activity), Lyman alpha flux (the best measure of solar activity in the top of the chromosphere and base of the transition region from the SME satellite) and the combined Mg II core-to-wing ratio from the NIMBUS7 and NOAA9 satellites for solar cycle 21 and the rise of cycle 22 (used here as being representative of the temporal shape of the UV flux variations in the 175 - 285 nm range, HEATH and SCHLESINGER, 1986; DONNELLY, 1988b). Notice the very flat background (excluding the occasional solar-rotational spike) in 1985 and 1986 in F10, a quite flat background but with a little more curvature in the Mg II UV data (with more numerous short-term spikes), and the even greater long-term curvature in the Lyman alpha data. So we see minor differences in the long-term variations or shape of the solar cycle among these three data sets. R(MgIIc/w) reached 60% higher in Jan. 1989 (not shown) than the highest values shown in mid 1988 relative to the solar minimum values in Sept. 1986, which is already as high as being just below the annual average for the peak of solar cycle 21. So we expect solar cycle 22 to have as strong or stronger UV and EUV emission as in cycle 21.

INTERMEDIATE-TERM VARIATIONS

Intermediate-term variations last from about 4 to 11 months and may be considered to be of two types. An example of the first type can be seen in all three data sets in Figure 2, peaking in early 1984 and lasting about 11 months. Other such variations are evident in 1982 and 1983. They are also present in 1978 - 1981, but one may want to smooth out the solar rotational variations to see them more clearly. Neglecting the short-term variations, notice how similar in temporal shape the intermediate-term variations are in these three data sets and how their amplitude relative to the solar cycle minimum-to-maximum amplitude is about the same. Notice that these intermedite-term variations are very weak or absent in F10 and quite weak in the Mg II UV data in 1985 and 1986 during solar cycle minimum but fairly strong throughout 1978 through mid 1984. These variations are related to increases and decreases in the number of active regions where the regions are widely distributed in solar longitude so that the average per rotation varies.

Figure 3 shows short-term solar rotational variations and a mixture of the two types of intermediate variations. The second type of intermediate variation involves a modulation of the solar-rotational amplitudes over a four to nine month interval. For example, after the tick marked May 30, there is a small rotational peak (at the time of a dip in S from sunspot darkening) followed by two giant ones and then three medium solar rotational peaks. That train of peaks spaced fairly evenly in time is then followed by new peaks at a different phase in the solar rotation. Note that the giant peak in July is partly so large because the amplitude of the rotational minima has been decreasing for several rotations. The two types of intermediate-term variations involve the same physical process of the emergence and evolution of groups of active regions; they are analogous to mathematically separating the longitudi-

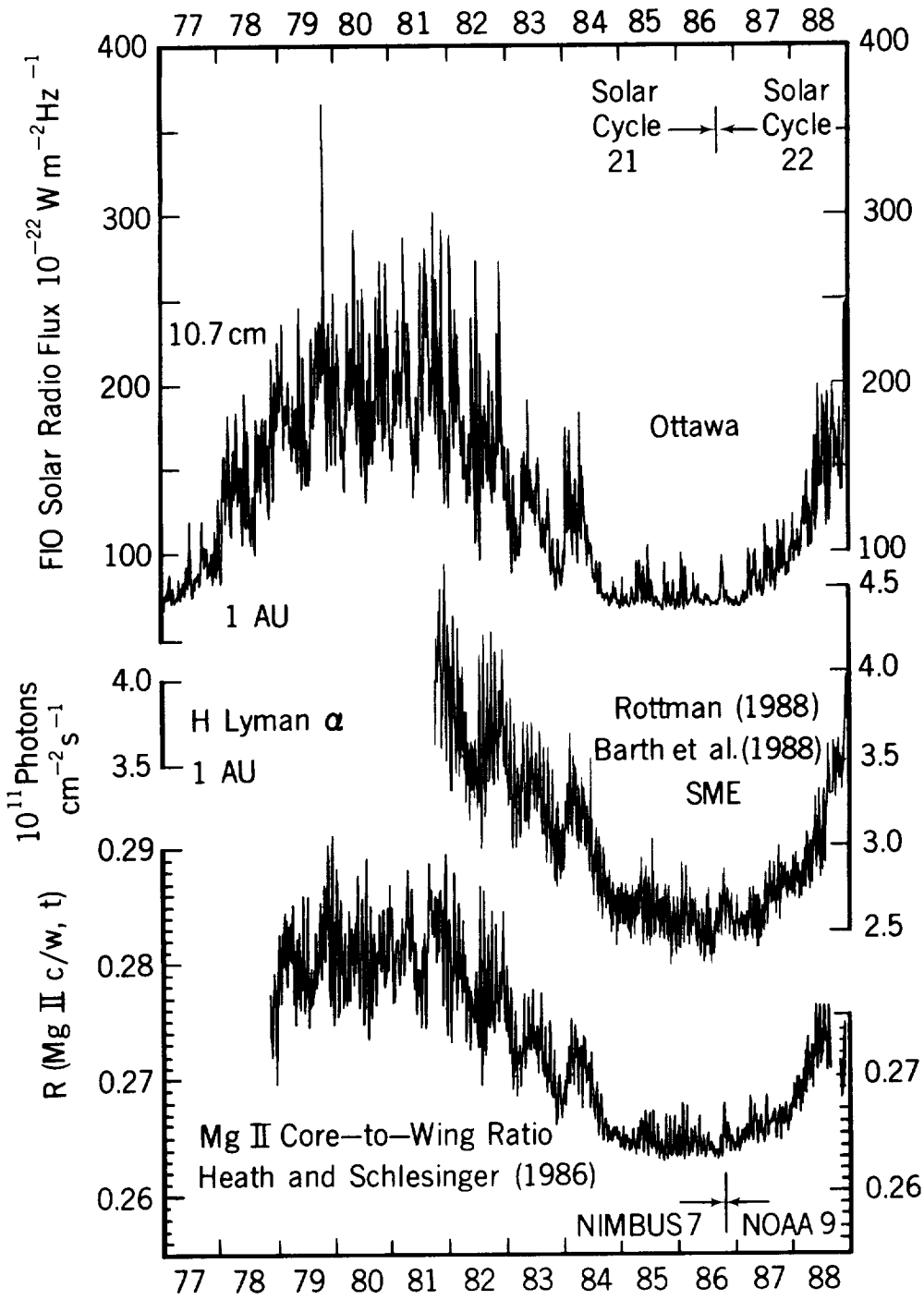

Figure 2. Solar cycle 21 and the rise of cycle 22 for F10, H Lyman alpha, and R(MgIIc/w), first from NIMBUS7 and then from NOAA9 after Oct. 1986.

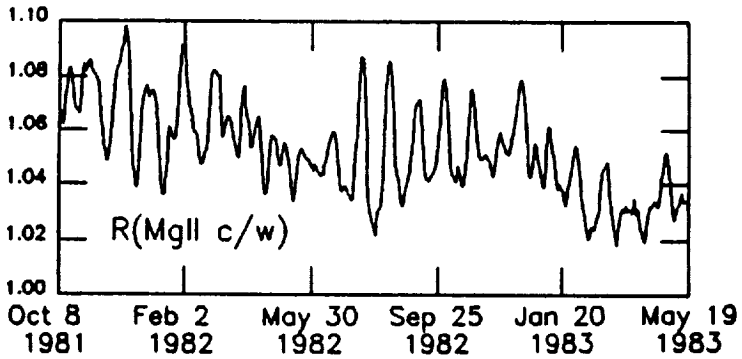

Figure 3. The NIMBUS7 Mg II core-to-wing ratio normalized to the monthly average of Sept. 1986 at the solar cycle minimum.

nal distribution of activity into a rotational average value and the deviations from the average. Sometimes two of the second type appear to form one of the first type as follows. For example, an episode of major activity emerged in August 1979. As the amplitudes of the rotational peaks rose and then decayed, the amplitude of the rotational minima steadily rose. Another episode of major activity then emerged in November 1979. While its rotational peaks rose and then decayed, the rotational minima also rapidly decreased in amplitude. See Figure 2. There is a tendency to think that rapid flux changes are only related with the emergence of new activity and the influence of plage remnants leads to slower decreases in flux. However, quite large decreases in flux do occur from one rotation to the next probably due to a rapid decrease in the rate of emergence of activity.

One difference in the two types of intermediate term variations is that for the second type, the amplitude modulation of the solar rotational variations caused by a major group of active regions, F10 rises more rapidly, peaks earlier and decays faster than for the UV fluxes (DONNELLY et al., 1983). For example, just above the dividing line between NIMBUS7 and NOAA9 data in Figure 2, one sees an isolated peak in F10 but several small subsequent solar rotational variations in Mg II and Lyman alpha. In 1985 and 1986, there are fewer solar-rotational peaks in F10 than in the UV data. Conversely, there is good agreement for F10, Lyman alpha and Mg II in the size and shape of the first type of intermediate-term variation relative to the solar-cycle amplitude.

So far, research of the atmospheric effects of solar UV variations has concentrated on the short-term variations because they were the first data available, the consequent effects in ozone and temperature could be clearly identified in stratospheric measurements, and interesting complications between the early model results and the observed effects were discovered. Analysis of these intermediate-term variations will likely be the next area of active research, although CHANDRA (1989) has shown it will be difficult to identify their stratospheric effects. Note that their durations vary significantly from one to another in Figure 2, i. e. they are not a simple periodicity.

SHORT-TERM VARIATIONS

Solar UV fluxes vary over days to weeks due to the evolution of active regions and the strong modulation caused by the combination of solar rotation and the strong decrease in UV flux emission with increasing solar central angle for the location of the region as viewed from Earth. The solar rotation modulation causes the time series in Figure 3 to be full of narrow peaks. The

fact that no two of these peaks are of equal amplitude or are identical in relative shape is a consequence of the combined effects of the temporal evolution of several active regions. Note that the amplitude of these short-term variations are quite large, frequently about as large as half the smoothed solar cycle increase. See Figure 2. The amplitude of the giant solar-rotational variation in the center of Figure 3 is more than 80% of the smoothed solar cycle amplitude. Figure 3 shows weak 13-day periodicity (two peaks per rotation) mixed with 27-day periodicity in March and April 1982, and in Dec. 1982 and Jan. 1983, which is a common occurrence in UV fluxes.

The short-term variations differ significantly in F10 relative to those in the UV flux, e. g. the lack of 13-day periodicity in F10, the faster rise, earlier peak and quicker decay in F10 of episodes of 27-day solar rotational variations caused by major groups of active regions (DONNELLY et al., 1983), a larger half-maximum width of the 27-day solar rotational variations for F10, and the larger amplitude of the short-term variations relative to the smoothed solar cycle amplitude in F10 (DONNELLY, 1987). Some authors refer to a good agreement between F10 and UV fluxes while others emphasize the disagreements; the former are usually refering to comparisons of long-term variations and the latter to short-term variations.

Mg II CORE-TO-WING RATIO

The short-term variations of the solar UV flux within the 175 - 285 nm range have been shown to be highly uniform in temporal shape, although the percentage amplitude varies with wavelength (HEATH and SCHLESINGER, 1986; DONNELLY, 1988b). This uniformity is interpreted to be caused by the solar central angle dependence of active region emission and the strength of one region relative to another as a function of time being uniform over this wavelength range because the source regions are essentially the same. This uniformity does not extend to all wavelengths, which is drastically evident in Figure 1. But within this limited wavelength range, the uniformity of souce regions and emission and absorption mechanisms suggests that the intermediate and long-term variations also have uniform temporal shapes, which is the assumption used when applying the Mg II core-to-wing ratio to estimate the long-term variations of the UV flux within the 175 - 285 nm range. Indeed, in the cases of F10 and Lyman alpha, where large and small differences, respectively, are known to occur for short-term variations with respect to the UV flux within the 175 - 285 nm range, the long- and intermediate-term variations for both F10 and Lyman alpha are fairly similar to those of the Mg II line in Figure 2.

GROUND-BASED MEASURES OF SOLAR ACTIVITY

The correlation coefficient for the NIMBUS7 or NOAA9 Mg II core-to-wing ratio with respect to the Ca K 1A index is about 0.98. It appears to be the best ground-based measure for estimating solar UV fluxes. Unfortunately, it is not available daily. The He I 10830 A data is probably not as closely related to the UV flux variations, but it is available almost daily and will be useful for occasionally estimating UV fluxes missing in the satellite measurements. F10 is useful for estimating the short-term variations of coronal EUV fluxes. For chromospheric EUV fluxes and chromospheric and upper photospheric UV fluxes, F10 is helpful for long-term and intermediate-term variations, but not for short-term variations. Figure 1 show that sunspot numbers are not very useful for estimating UV flux variations. The calcium plage index is helpful only for short-term variations; it fails for intermediate- and long-term variations because of numerous small bright features not included in the scaled data that are important for the UV flux. Digitized raster-scans of the solar disk in the Ca-K line should overcome the shortcomings in the older plage index.

CONCLUSIONS

Twenty years ago, we knew the general spectral shape of solar UV fluxes but not much about their temporal variations. Today, several satellites provide daily solar UV measurements and better instruments will soon be flown. (It is amazing there are no monitoring measurements of the solar EUV flux below 115 nm!) Short-term variations are very well measured and fairly well modelled. Intermediate-term variations are the next active area for intercomparing different satellite measurements, modeling the UV fluxes and researching their stratospheric effects.

REFERENCES

Barth, C.A., W.K. Tobiska, and G.J. Rottman, Comparison of the solar Lyman alpha flux with the solar 10.7 cm radio flux, EOS, 69, 1354, 1988.

Chandra, S., Response of the middle atmosphere to solar and dynamical perturbations, this volume, 1989.

Donnelly, R.F., D.F. Heath, J.L. Lean and G.J. Rottman, Differences in the temporal variations of solar UV flux, 10.7-cm solar radio flux, sunspot number, and Ca-K plage data caused by solar rotation and active region evolution, J. Geophys. Res., 88, 9883, 1983.

Donnelly, R.F., Temporal trends of solar EUV and UV full-disk fluxes, Solar Phys., 109, 37-58, 1987.

Donnelly, R.F., The solar UV Mg II core-to-wing ratio from the NOAA9 satellite during the rise of solar cycle 22, Adv. Space Res., 8, (7)77-(7)80, 1988a.

Donnelly, R.F., Uniformity in solar UV flux variations important to the stratosphere, Annales Geophys., 6, 417-424, 1988b.

Heath, D.F., A review of observational evidence for short and long term ultraviolet flux variability of the sun, Sun and Climate, CNES, 18 Ave. Edouard - Belin, 31055 Toulouse Cedex, France, 447-471, 1980.

Heath, D.F., and B.M. Schlesinger, The Mg 280-nm doublet as a monitor of changes in solar ultraviolet irradiance, J. Geophys. Res. **91**, 8672, 1986.

Hickey, J.R., B.M. Alton, H.L. Kyle, and D. Hoyt, Total solar irradiance measurements by ERB/NIMBUS-7. A review of nine years, Space Sci. Rev., 48, 321-342, 1988.

Labs, D., H. Neckel, P. C. Simon and G. Thuillier, Ultraviolet solar irradiance measurement from 200 to 358 nm during Spacelab 1 mission, Solar Phys., 107, 203-219, 1987.

Lean, J.L., O.R. White, W.C. Livingston, D.F. Heath, R.F. Donnelly, and A. Skumanich, A three-component model of the variability of the solar ultraviolet flux: 145-200 nM, J. Geophys. Res., 87, 10307-10317, 1982.

Rottman, G.J., Observations of solar UV and EUV variability, Adv. Space Res., 8, (7)53-(7)66, 1988.

Rottman, G.J., C.A. Barth, R.J. Thomas, G.H. Mount, G.M. Lawrence, D.G. Rusch, R.W. Sanders, G.E. Thomas and J. London, Solar spectral irradiance, 120 - 190nm, October 13, 1981 - January 3, 1982, Geophys. Res. L., 9, 587, 1982.

Rybansky, M., V. Rusin, and E. Dzifcakova, Coronal index of solar activity, V. Years 1977-1986, Bull. Astron. Inst. Czechosl., 39, 106-119, 1988.

Schatten, K.H., A model for solar constant secular changes, Geophys. Res. L., 15, 121-124, 1988.

VanHoosier, M.E., J.-D.F. Bartoe, G.E. Brueckner, D.K. Prinz, and J.W. Cook, A high precision solar ultraviolet spectral irradiance monitor for the wavelength region 120-400 nm, Sol. Phys., 74, 521-530, 1981.

Wagner, W.J., Observations of 1-8A solar x-ray variability during solar cycle 21, Adv. Space Res., 8, (7)67-(7)76, 1988.

Wilson, R.M., D. Rabin, and R.L. Moore, 10.7-cm solar radio flux and the magnetic complexity of active regions, Solar Phys., 111, 279-285, 1987.